Proceedings of the 9th World Congress on Mechanical, Chemical, and Material Engineering (MCM'23)
Brunel University, London, United Kingdom - August 06-08, 2023
Paper No. ICMIE 143
DOI: 10.11159/icmie23.143

Fracture Behavior Prediction of a High-Strength Aluminum Alloy under Multiaxial Loading

Eray Arslan[1], Mehmet Haskul[2]
[1]Vienna University of Technology
Institute for Mechanics and Mechatronics, Vienna, Austria
eray.arslan@tuwien.ac.at
[2]Şırnak University
Department of Mechanical Engineering, Şırnak, Turkey
mehmethaskul@sirnak.edu.tr

Abstract - This study presents a triaxiality analysis and fracture behavior prediction of a high-strength aluminum alloy, specifically AW5754, under multiaxial loading conditions. The primary objective is to obtain a triaxiality locus, which depicts the relationship between the equivalent plastic strain to fracture and the stress triaxiality factor. This locus provides comprehensive insights into the fracture behavior of the material under various stress states. Experimental tests employing various specimen geometries are conducted to acquire essential data for analysis and to facilitate the development of a finite element (FE) model. Quasi-static uniaxial tensile tests are performed on five different specimen types, and accurate deformation measurements are obtained using extensometers at critical locations. The simulation results from the FE models are then compared with the experimental measurements to ensure their accuracy. The developed FE models are used to calculate the equivalent fracture strain and stress triaxiality factor with the help of collected test data. These calculations enable the generation of a stress triaxiality locus through a curve-fitting process. An exponential curve fitting function is chosen to appropriately relate the equivalent plastic strain to the fracture and stress state for the AW5754 aluminum alloy. The resulting stress triaxiality locus serves as a valuable tool for predicting fracture strain and evaluating stress states more accurately. The outcomes of this study contribute significantly to our understanding of the fracture behavior exhibited by high-strength aluminum alloys under multiaxial loading conditions.

Keywords**:** High-strength aluminum alloys, multiaxial loading, triaxiality locus, fracture behavior, finite element simulation.

1. Introduction

High-strength aluminum alloys are widely used in numerous engineering applications due to their desirable properties, such as their lightweight construction, excellent corrosion resistance, and the high strength-to-weight ratio [1]. These alloys find extensive use in the fabrication of tread plates, automotive components, and ship parts, among others [1]. These materials are often subjected to complex multiaxial loading conditions, which can lead to ductile fracture [2]. Accurately detecting fracture locations within intricate structures and estimating corresponding failure loads are of paramount importance to designers and engineers. While determining uniaxial fracture strain through standard tensile tests using simple specimens is relatively straightforward, predicting multiaxial fracture behavior based on these tests presents significant challenges. Moreover, the fracture strain obtained from such standard specimens may not accurately reflect the behavior under multiaxial loading conditions. Therefore, it is crucial to establish a stress triaxiality locus [3] that provides comprehensive insights into fracture strain as it relates to the multiaxial stress state of the material.

The triaxiality locus, a graphical representation correlating equivalent plastic strain to fracture with the stress triaxiality factor (TF), is a valuable tool for understanding the fracture behavior of materials across various stress states [4]. Establishing the triaxiality locus for a specific material makes it possible to obtain detailed insights into its fracture behavior under diverse stress conditions, thereby facilitating more accurate predictions. Figure 1 illustrates different regions on the locus, each representing a unique stress state. Within these regions, fracture points corresponding to different specimen geometries and loading conditions are identified, and curves are fitted through these points. The fracture points are determined using uniaxial or biaxial tensile or compressive test measurements that are relevant to each specific case.

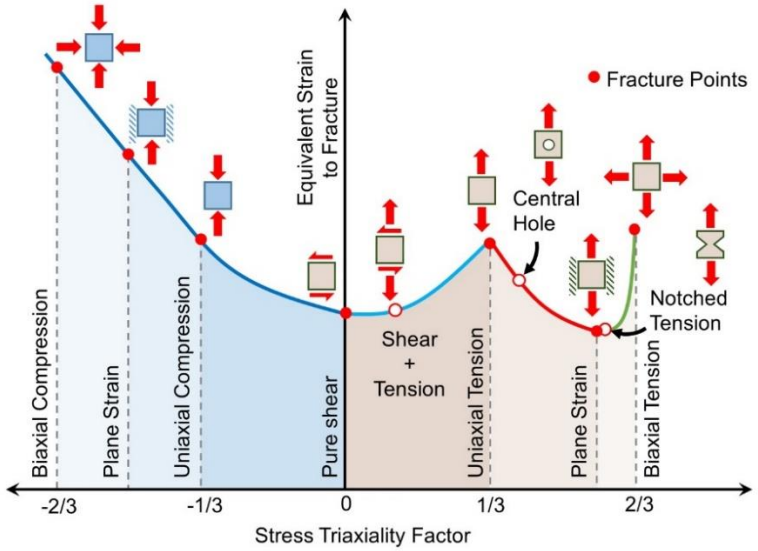

Fig. 1: A sample of the stress triaxiality locus for a ductile material (adapted from [5, 6])

TF is defined as the ratio of the hydrostatic stress to the equivalent stress (von Mises in our case) and calculated by the following equation [7]

$$TF = \frac{(\sigma_1 + \sigma_2 + \sigma_3)/3}{\sqrt{[(\sigma_1 - \sigma_2)^2 + (\sigma_2 - \sigma_3)^2 + (\sigma_3 - \sigma_1)^2]/2}} \tag{1}$$

where σ_i are principal stresses.

To obtain a comprehensive triaxiality locus, it is necessary to perform experiments that include a range of stress states [3]. However, performing tests for all data points in the locus is very expensive [8]. Therefore, it is recommended in the existing literature to conduct a minimum of four tests, such as for uniaxial tension, pure shear, combined shear-tension, and notched specimens, and subsequently fit the test data to obtain the locus curve [8]. Previous studies examine similar analyses for different materials, including steels and aluminum alloys, in references [3, 5, 7, 9-13]. The fracture behavior and the corresponding finite element (FE) model have been investigated for AW5754 in a separate study [14]. Specifically, uniaxial tensile tests were performed on AW5754 specimens to observe the deformation behavior and cross-section reduction. In addition, a methodology for determining material characteristics in high-speed forming processes involving AW5754 has been developed [15]. Nevertheless, a thorough analysis of the stress triaxiality locus for AW5754 under quasi-static loading conditions has yet to be reported in the existing literature.

The present study focuses on conducting a stress triaxiality analysis of the AW5754 aluminum alloy to evaluate the stress state of structures subjected to complex loading conditions and facilitate the prediction of fracture strain under multiaxial stress states. To accomplish the objectives of this study, a series of quasi-static uniaxial tensile tests are conducted using five different types of test specimens with varying geometries. These include standard tensile specimens, pure shear specimens, shear-tensile specimens (45°), notched specimens, and centrally drilled specimens. The use of extensometers ensures precise measurement of deformations at critical locations. The acquired experimental data is then employed to identify initial fracture locations, establish their correlation with corresponding loads and validate the results of FE simulations. Based on the test results, FE models are developed to determine data points for fracture strain and stress triaxiality factor [16]. These models facilitate the calculation of equivalent plastic fracture strain and the triaxiality factor at specific measurement areas within the tests. Subsequently, using a curve fitting process, these data points are utilized to generate a stress triaxiality locus for the material. Various mathematical functions have been

proposed in the literature for curve fitting to obtain the triaxiality locus [8]. Nevertheless, it is crucial to emphasize that selecting these functions depends on the material properties and its characteristic behavior under different loading conditions. conditions. In this study, an exponential fitting function is chosen for this process as it effectively establishes the appropriate appropriate relationship between equivalent plastic strain to fracture and the stress state for the AW5754.

2. Experimental Methodology

A series of quasi-static uniaxial tensile tests is performed on five different types of test specimens with varying geometries. These specimens include standard tensile (Specimen I), pure shear (Specimen II), shear-tensile (Specimen III), notched (Specimen IV), and centrally drilled (Specimen V) specimens, as shown in Figure 2. The specimens are manufactured by laser cutting from AW5754 aluminum sheet with a thickness of 3 mm.

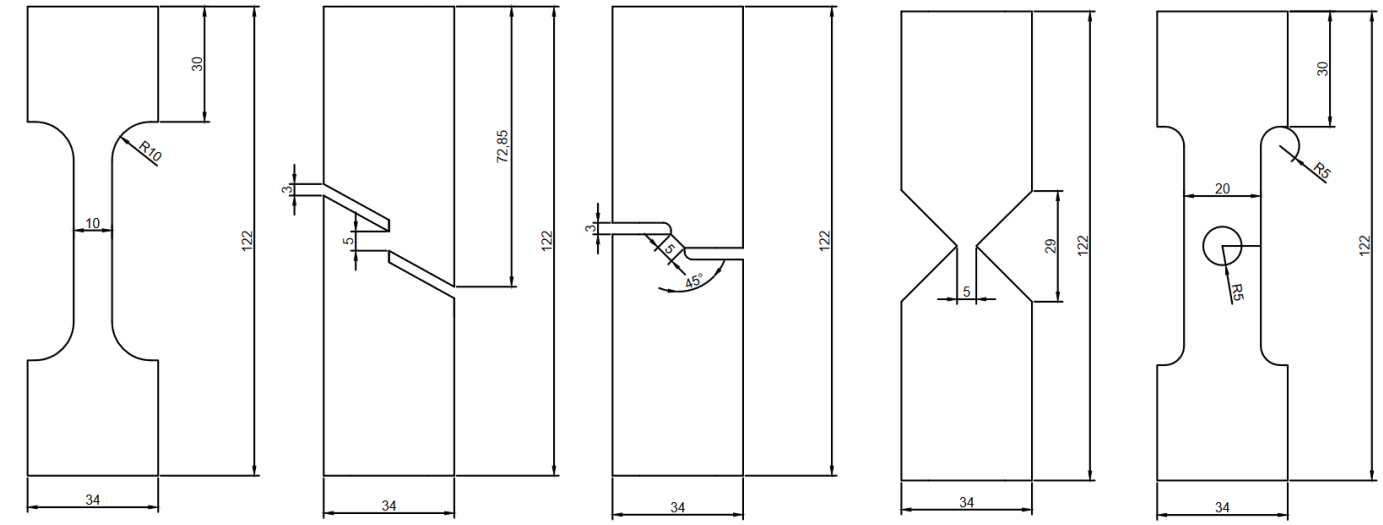

Specimen I (uniaxial tension) | Specimen II (pure shear) | Specimen III (shear-tension-45°) | Specimen IV (notched) | Specimen V (centrally drilled)

Fig. 2: Specimen geometries

The tests are performed on three samples for each specimen type, and measurements are recorded. These displacement-control tensile tests are performed at a 1 mm/min speed. Accurate deformation measurements at critical locations on each sample are achieved using extensometers. The test machine's head applies the axial tensile load, and each sample's displacement between extensometers is also measured (see Figure 5). During the tests, loading is applied until the fracture of the entire samples, as this analysis focuses explicitly on fracture strain and its corresponding stress state. True stress and logarithmic strains are calculated only for Specimen type I, corresponding to the standard tensile test specimen, and plotted in Figure 3. This plot also facilitates the calculation of the material's modulus of elasticity (70 GPa) and yield stress (110 MPa). The test results further contribute to defining the stress-plastic strain relation, capturing the alloy's hardening behavior. The material data in the plastic regions derived from these test results are employed in all FE simulations, including Specimens II-V. It is important to note that while a true stress-strain curve can be plotted for Specimen I, calculating stresses and strains for the deformed bodies of the other specimen types without FE models is challenging. Hence, force-displacement (between extensometers) curves are plotted for Specimens II-V (Figure 5) and used for further FE analysis. These data are utilized to verify the subsequent FE models and detect the fracture points in the corresponding specimens.

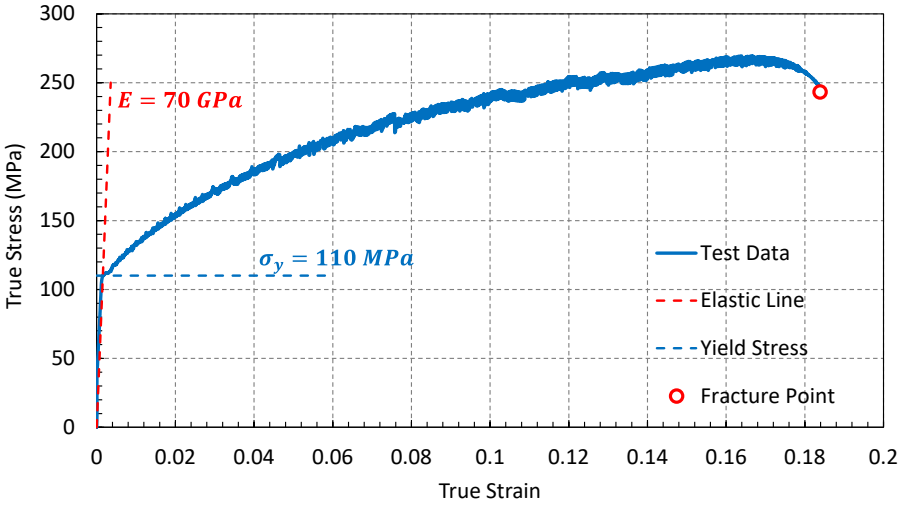

Fig. 3: True stress-strain curve for Specimen I

3. Finite Element Simulation

Equivalent plastic strain to fracture and evolution of the stress triaxiality factor should be detected to define the triaxiality locus for the ductile material. While these response variables can be theoretically calculated for specimen types I-III based on various assumptions [7], achieving more realistic results necessitates analysing finite element (FE) models, considering the highly nonlinear deformation behavior of the material under multiaxial loading, particularly beyond the necking region. Consequently, in this study, FE models are developed in ABAQUS for each specimen type and loading conditions. The validity of these FE models is first confirmed by comparing them with the corresponding test results. Subsequently, the models are utilized to establish the relationship between equivalent plastic strain to fracture and the stress triaxiality factor.

Figure 4(a) presents a representative sample for the FE model, specifically for Specimen type I. One-quarter of the specimen is meshed with two planes of symmetry, accounting for its symmetrical geometry and uniform loading conditions. The reference point depicted in the figure corresponds to the control point of the model, which is used to apply input axial displacement along the x-direction. This reference point is kinematically coupled to the loading surface, representing the contact surface between the specimen and the head of the tensile test machine in the experiments. This coupling ensures the uniform distribution of the applied input axial displacement on this surface. Moreover, it is crucial to identify the fracture measurement point, which indicates the fracture initiation location, for each specimen type. In the case of Specimen I, this critical point is also indicated in Figure 4(a). For the remaining specimen types, thorough examination of the experiments and deformed test samples is conducted to identify corresponding nodes in the FE model.

The modulus of elasticity, yield stress, and non-linear hardening behavior of the material are defined for all specimen types using the data provided in Figure 3, which was prepared specifically for Specimen type I. However, no damage behavior is incorporated into the FE model. During the simulation of the FE model, various outputs are obtained. As an example, Figure 4(b) illustrates the distribution of equivalent plastic strain in the sample.

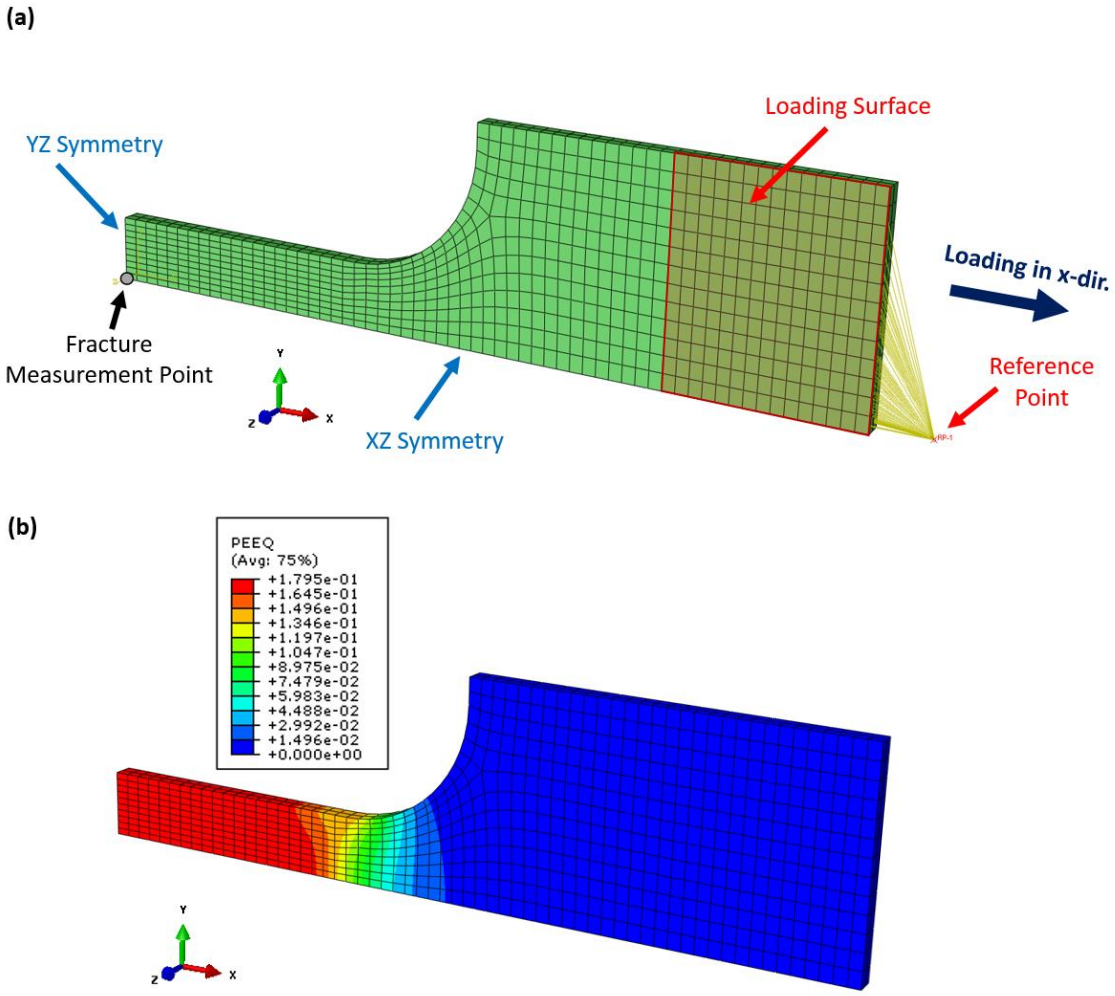

Fig. 4: (a) FE Model and (b) Equivalent plastic strain distribution in the specimen

FE model simulations are performed, and the force-displacement relationships are compared with the test results, as depicted in Figure 5(a-e). These figures show that the FE simulations yield reasonable outcomes, thereby validating their accuracy. It is important to note that the FE models do not include any damage models, and therefore, they are unable to identify the initiation of specimen fracture. Consequently, in the experimental tests, the fracture initiation points are determined and considered as the termination criteria for the simulations. Accordingly, equivalent plastic strains and stress triaxiality factors are calculated in the FE Model up to these fracture points, and their corresponding values are presented in Figure 5(f).

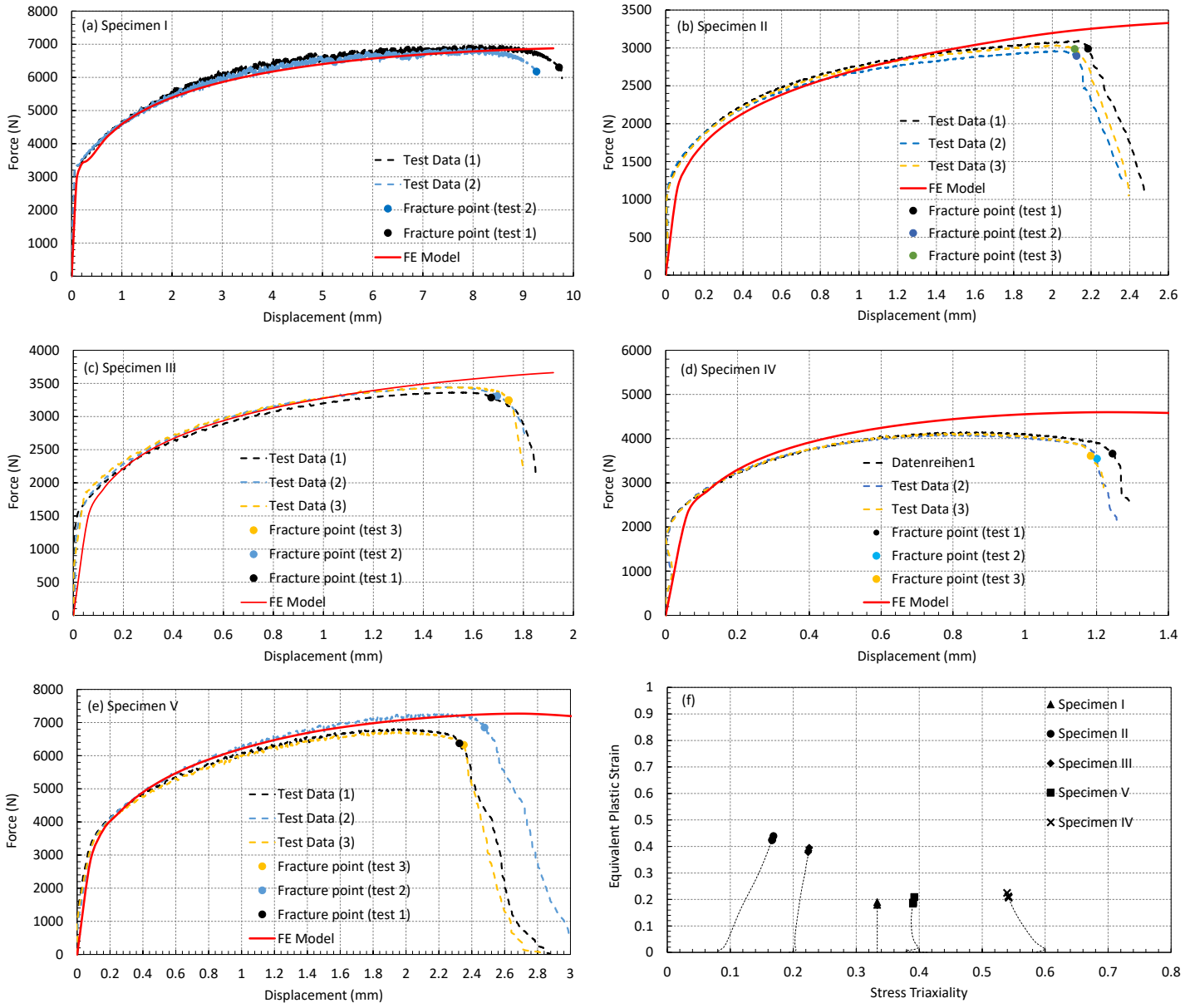

Fig. 5. Comparison of test data and FE Simulations and defined fracture points for (a) Specimen I, (b) Specimen II, (c) Specimen III, (d) Specimen IV, (e) Specimen V; (f) Change of equivalent plastic strain with stress triaxiality factor

4. Triaxiality Locus

To establish a continuous curve representing the triaxiality locus, the data points for each specimen in Figure 5(f) are subjected to a fitting process. For this fitting procedure, this data and the following exponential function are used [17, 18]

$$\epsilon_p^f = D_1 + D_2\, e^{D_3\, TF} \tag{2}$$

where TF denotes the stress triaxiality factor, and D_i are constants. The values of these constants in the function are determined by minimizing the error between the function and the data points. The resulting curve, accompanied by the calculated values of the constants D_i, is presented in Figure 6.

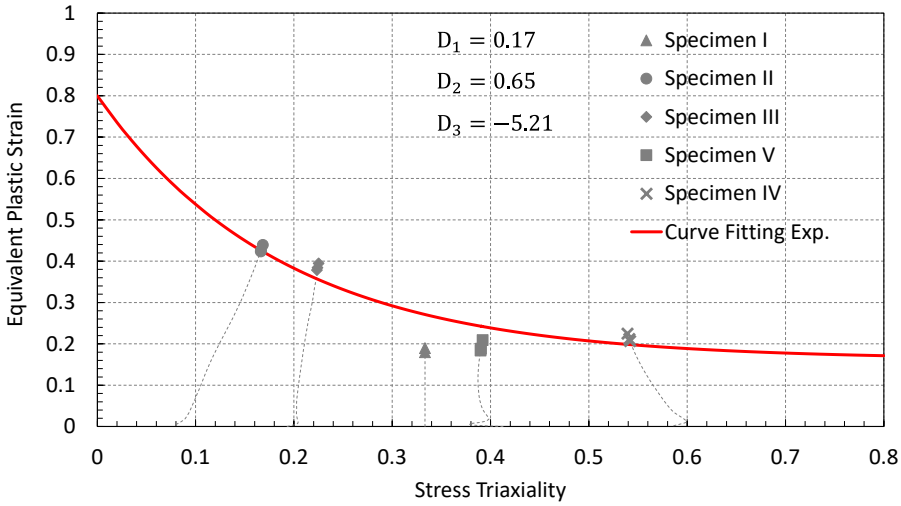

Fig. 6: Stress triaxiality locus for AW5754

5. Conclusion

Five different types of test specimens are subjected to uniaxial monotonic tensile tests. The tested specimens comprised the classical rectangular cross-sectional uniaxial test specimen, a pure shear specimen, a combined shear and tensile specimen (with a 45° angle), a notched specimen, and a specimen with a hole. The obtained test results are used to validate the corresponding FE simulations under similar loading conditions and to determine the critical load and strain necessary for the fracture of the entire specimen. Subsequently, FE simulations are carried out to compute the equivalent plastic strain and the stress triaxiality factor for each specimen type. The resulting data points are then utilized to fit and obtain a comprehensive triaxiality locus for the material AW5754.

In the finite element model, multiple nodes are controlled to accurately identify a representative node that corresponds to the measurement point in the tests. The findings presented in this study specifically pertain to the final outcomes; therefore, the results for other nodes are not included.

In the process of fitting the data, various functions are suggested in the literature [8]. Although a general triaxiality locus is defined in the Introduction (see Figure 1), it should be acknowledged that each material exhibits a different characterization regarding its fracture resistance. For instance, cast aluminum materials generally have higher shear fracture strains compared to their tensile fracture strains. Therefore, it is crucial to select a function that is most suitable for capturing the specific behavior of the studied material. In the case of AW5754, the exponential function is the most appropriate for fitting the obtained data.

Acknowledgements

This study is financially supported by Sirnak University (under the project number 2022.FNAP.06.05.02) and TU Wien.

References

[1] T. Trzepieciński, S. M. Najm, V. Oleksik, D. Vasilca, I. Paniti, M. Szpunar, “Recent developments and future challenges in incremental sheet forming of aluminium and aluminium alloy sheets,” *Metals*, vol. 12, no. 1, pp. 124, 2022.

[2] P. Foti, S. M. J. Razavi, A. Fatemi, F. Berto, "Multiaxial fatigue of additively manufactured metallic components: A review of the failure mechanisms and fatigue life prediction methodologies," *Progress in Materials Science*, vol.137, pp. 101126, 2023.
[3] Y. Bao, T. Wierzbicki, "On fracture locus in the equivalent strain and stress triaxiality space," *International Journal of Mechanical Sciences*, vol. 46, no: 1, pp. 81-98, 2004.
[4] P. W. Bridgman, *Studies in Large Plastic Flow and Fracture: with Special Emphasis on the Effects of Hydrostatic Pressure*, Harvard University Press, 1964.
[5] M. Kõrgesaar, "The effect of low stress triaxialities and deformation paths on ductile fracture simulations of large shell structures," *Marine Structures*, vol. 63, pp. 45-64, 2019.
[6] Z. A. Mehari, J. Han, "Numerical prediction of ductile fracture during the partial heating roll forming process of DP980," *International Journal of Fracture*, vol. 234, no: 1-2, pp. 97-112, 2022.
[7] Y. Peng, X. Chen, S. Peng, C. Chen, J. Li, G. Liu, "Strain rate-dependent constitutive and low stress triaxiality fracture behavior investigation of 6005 Al alloy," *Advances in Materials Science and Engineering*, vol. 2018, ID 2712937, 2018.
[8] M. Asadi, F.H. Aboutalebi, M. Poursina, "A comparative study of six fracture loci for DIN1623 St12 steel to predict strip tearing in a tandem cold rolling mill," *Archive of Applied Mechanics*, vol. 91, no. 4, pp. 1859-1878, 2021.
[9] M. Kõrgesaar, J. Romanoff, H. Remes, P. Palokangas, "Experimental and numerical penetration response of laser-welded stiffened panels," *International Journal of Impact Engineering*, vol. 114, pp. 78-92, 2018.
[10] L. Zhou, H. Wen, "A new dynamic plasticity and failure model for metals," *Metals*, vol. 9, no. 8, pp. 905, 2019.
[11] H. Mae, X. Teng, Y. Bai, T. Wierzbicki, "Comparison of ductile fracture properties of aluminum castings: Sand mold vs. metal mold," *International Journal of Solids and Structures*, vol. 45, no. 5, pp. 1430-1444, 2008.
[12] L. Fraccaroli, M. N. Mastrone, F. Concli, "Calibration of the Fracture Locus of an AlSi10 Aluminum Alloy," *WIT Transactions on The Built Environment*, vol. 196, pp. 3-10, 2020.
[13] H. Mae, X. Teng, Y. Bai, T. Wierzbicki, "Ductile fracture locus of AC4CH-T6 cast aluminium alloy," *Archives of Computational Materials Science and Surface Engineering*, vol. 1, no. 2, pp. 100-105, 2009.
[14] P. Kumar, "Experimental and extended finite element simulations for tensile fracture phenomenon of cryorolled aluminium alloy 5754," *Proceedings of the Institution of Mechanical Engineers, Part C: Journal of Mechanical Engineering Science*, vol. 236, no. 5, pp. 2488-2498, 2022.
[15] V. Psyk, C. Scheffler, M. Tulke, S. Winter, C. Guilleaume, A. Brosius, "Determination of material and failure characteristics for high-speed forming via high-speed testing and inverse numerical simulation," *Journal of Manufacturing and Materials Processing*, vol. 4, no. 2, pp. 31, 2020.
[16] F. Andrade, S. Conde, M. Feucht, M. Helbig, A. Haufe, "Estimation of stress triaxiality from optically measured strain fields," in *Proceedings of the 12th European LS-DYNA Conference*, Koblenz, Germany, pp. 14-16, 2019.
[17] J. R. Rice, D. M. Tracey, "On the ductile enlargement of voids in triaxial stress fields," *Journal of the Mechanics and Physics of Solids*, vol. 17, no. 3, pp. 201-217, 1969.
[18] Y. Abushawashi, X. Xiao, V. Astakhov, "A novel approach for determining material constitutive parameters for a wide range of triaxiality under plane strain loading conditions," *International Journal of Mechanical Sciences*, vol. 74, pp. 133-142, 2013.